Tellus (1987), *39A*, 152–160

Results of extensive integrations with simple NWP models over the tropics during FGGE

By T. N. KRISHNAMURTI, ARUN KUMAR and XIANG LI, *Department of Meteorology, Florida State University, Tallahassee, FL 32306, USA*

(Manuscript received May 19, 1985; in final form September 15, 1986)

ABSTRACT

In this note, we present a summary of results from a total of some 980 forecast experiments made with two simple high-resolution regional models. The models are based on the principles of conservation of absolute vorticity (a streamfunction barotropic model) and of potential vorticity (the shallow water equations with bottom topography). These regional forecast models are applied to a number of different domains (winter monsoon, central Pacific Ocean during Northern winter, Central America, Eastern Atlantic and South America, West African Monsoon, Indian summer monsoon and summer monsoon over Southeast Asia). The data sets for these experiments are those derived from the First GARP Global experiment (FGGE), the Asian Monsoon experiment (MONEX) and the West African monsoon experiment (WAMEX). Statistical evaluation includes a comparison of the root mean square vector wind error with the corresponding persistence errors. The results of this study show that these models have a varied skill over different domains. The single-level primitive equation model over West Africa, South America and the Atlantic Ocean during northern summer shows a skill beyond the persistance for a range of 4 days of integration. The performance of the single-level primitive model appears quite promising over these regions. These long series of experiments with the single-level primitive equation model were carried out with the choice of the mean free surface height of 2 km with a maximum height of the orography of 1 km.

A further effort at the optimization of the single level model was explored. Here, a parameter space consisting of the free surface height and the maximum height of the orography was explored in order to assess the skill of the vector wind error. Marked improvement in skill was noted over a domain centred over China from an optimization of these parameters.

1. Introduction

In this short note, we present a summary of results from a large number of (a total of around 980) regional numerical weather prediction experiments made with two simple models (see Krishnamurti and Pearce, 1977). The models are based on the conservation of absolute vorticity and of potential vorticity. These applications utilize FGGE data sets over several regional tropical domains during the northern summer and the winter season. (A list of acronyms is presented in Table 1.)

The motivation for this study was based on the following factors.

(a) Availability of global high resolution cloud motion vectors from five geostationary satellites during the global experiments and its sub-programs MONEX and WAMEX.

Table 1. *List of acronyms*

ECMWF	European Centre for Medium Range Weather Forecast
FGGE	First GARP Global Experiment
GARP	Global Atmospheric Research Programme
MONEX	Monsoon Experiment
NOAA	National Oceanic and Atmospheric Administration
PE	Primitive Equation
WAMEX	West African Monsoon Experiment
III-b	Analysed FGGE gridded data of many variables at many levels produced by ECMWF

(b) The availability of the FGGE IIIb analysis, (here we have used those based on ECMWF).

(c) The need to assess the performance of single level models over several tropical domains in the context of these best available data sets.

A number of domains were selected from phenomenological and regional interest (see Fig. 1).

I. Winter monsoon domain over Southeast Asia.
II. A Central Pacific domain during northern winter.
III. A Central American domain during northern summer.
IV. A Western Atlantic–South American domain during northern summer.
V. West African Monsoon—including the regions of easterly waves over the Atlantic Ocean.
VI. A summer monsoon domain over Arabian Sea and India.
VII. A summer monsoon domain over Southeast Asia.

An appealing aspect of these models is that they can be run operationally utilizing fairly small computers. The present series of experiments were run on a computer with the following specifications:

(a) memory 528 kilobytes
6 megabyte virtual memory
(b) disk drive 80 megabyte storage

The single-level models described in the following section utilize a horizontal resolution of roughly 100 km^2. An absolute vorticity conserving model utilizing some 2500 grid points can be integrated to 4 days using about an hour of computer time. The corresponding time for the shallow water-single level primitive equation model with bottom topography is around 3 h. These integrations were performed on a slow (0.1 MIPS) computer.

2. An outline of the models

2.1. *The non-divergent barotropic model*

This model is based on the principle of conservation of absolute vorticity which can be expressed as:

$$\frac{\partial}{\partial t}\nabla^2\psi = -J(\psi, \nabla^2\psi) - \beta\frac{\partial\psi}{\partial x}. \quad (1)$$

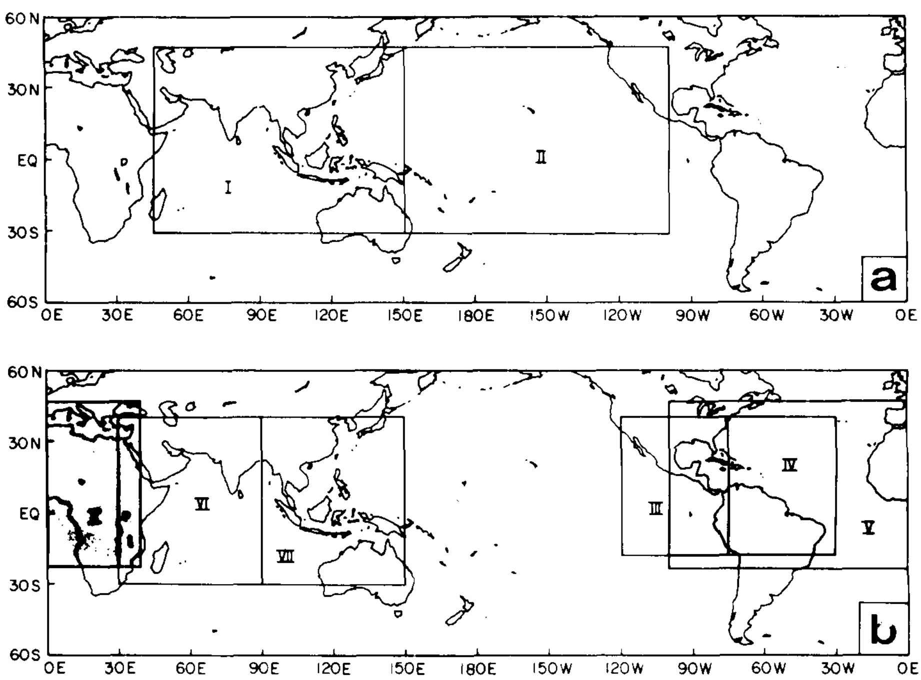

Fig. 1. Domain of experiments (a) northern winter season (b) northern summer season.

It can also be shown that inside a close domain, the total kinetic energy and all the integral powers of absolute vorticity ζ_a^n are conserved by (1). Based on these constraints the finite difference analogs of the horizontal derivatives in eq. (1) are written in such a way so as to conserve the domain averages of ζ_a, ζ_a^2 and k. This is achieved by evaluating the Jacobian in (1) by a method proposed by Arakawa (1966). This method at the same time prohibits the nonlinear computational instability arising from the nonlinear advection term. The time integration in the model is accomplished via an Euler backward time differencing scheme (Matsuno, 1966).

The initial distribution of stream function ψ is obtained by solving the Poisson equation $\nabla^2\psi = \partial u/\partial y - \partial v/\partial y$, where u and v are the given zonal and meridional wind components respectively. Prior to solving the Poisson equation for ψ, the initial u and v are modified in such a way so as to give zero net mass flux across the boundaries of the domain. The east-west boundaries in the numerical model are rendered cyclic by an addition of 6 additional rows beyond the eastern boundary. The ψ at these points were obtained by a cubic spline interpolation subject to the condition that the value of ψ at the new eastern boundary is equal to the value at respective grid point at the western boundary. During the time integration the streamfunction ψ is kept fixed, i.e., $\partial\psi/\partial t = 0$, at the north and south boundaries.

2.2. *The single level primitive equation model*

This model, which allows divergent motions, is based on the shallow water equations (e.g., see Pedlosky, 1979):

$$\frac{Du}{Dt} = fv - g\frac{\partial}{\partial x}(z+h),$$

$$\frac{Du}{Dt} = fu - g\frac{\partial}{\partial y}(z+h),$$

$$\frac{Dz}{Dt} = -z\left(\frac{\partial u}{\partial x} + \frac{\partial v}{\partial y}\right). \quad (2)$$

Where the left-hand side denotes a total derivative following the horizontal motion of the parcel.

The domain invariants of this model are the potential vorticity defined as $(\zeta + f)/z$, a total energy parameter $E = zk + \frac{1}{2}gz + gh$ and the mean free surface height $\bar{z}$. Again to avoid the nonlinear computational instability a semi-Lagrangian advection scheme, as proposed by Krishnamurti (1962) and Mathur (1970) has been used. This method avoids the explicit calculation of the nonlinear advection terms in the set of equations given above. The initial value of the free surface height z is obtained by solving the so called nonlinear balance equation. This is expressed by,

$$g\nabla^2 z = \nabla\cdot f\nabla\psi + 2J\left[\frac{\partial\psi}{\partial x}, \frac{\partial\psi}{\partial y}\right]. \quad (3)$$

Since the phase velocity of the gravity waves, relative to the mean flow, for the shallow waters is given by:

$$c - \bar{u} = \pm\sqrt{gz}. \quad (4)$$

The choice of mean surface height $\bar{z}$ is quite important. Based on earlier studies (Williamson, 1976; Ploshay, 1977) $\bar{z}$ for 700 mbs was assumed to be 2000 m. The bottom topography is normalized to a maximum value of 1000 m. This normalized topography is further smoothed so as to remove any sharp gradients. The optimization of these parameters is addressed in Section 4.

Although both the mass and the motion field data were available from the ECMWF, in order to have a self-consistant regional single level model the mass field was obtained from an initialization. To bring the initial mass and wind field in the balance, a dynamical initialization procedure was deployed. This entails a forward-backward integration in time and requires a number of iterations. Due to the frequency dependent damping property of the Euler backward time differencing scheme, the amplitude of high frequency gravity waves, which exists because of the imbalance between the mass and wind field, diminishes during the dynamical initialization procedure. Thus the mass and wind fields attain near balanced conditions at the beginning of the actual forecast. For further details on these single level models reference may be made to Krishnamurti and Pearce (1977), Krishnamurti et al. (1980) and Adejokun and Krishnamurti (1983).

During the time integration the u, v and z are kept constant at the north and south boundaries.

3. Summary of results

The summary of the root mean square vector wind errors and the persistance errors are presented in Tables 2 and 3. The table includes the regions, the domain, the period, forecast hours, the errors for the barotropic and the single level primitive equation model and the persistance errors. For each day of the indicated period a 96-h forecast was carried out at the 700 mb level for each of the two models.

As may be seen from column 4 of these 2 tables, the simple barotropic model does not have much skill over most of the tropics except for the West African monsoon region (domain V) which also includes the Eastern Atlantic Ocean. In this region this simple model has a skill beyond that of persistance for about 2 days. Over most regions the skill is less than 24 h. Over West Africa, the low-level easterly jet around 600 mb is known to be barotropically unstable (Rennick, 1976). The African waves over this region receive energy

Table 2. *Root mean square vector wind errors (winter) (Winter Monsoon, Pacific Ocean Domain)*

Region	Domain/period	Forecast hour	Barotropic model	One-level PE model	Persistence
I	41.25°E–150°E	24	4.9	5.3	4.9
winter monsoon	30°S–45°N	48	6.0	6.4	5.9
	1 Dec 1978	72	7.0	7.4	6.4
	19 Jan 1979	96	7.7	8.1	6.6
II	150°E–101.25°W	24	6.6	6.2	6.4
central Pacific	30°S–45°N	48	8.9	8.2	8.4
ocean domain	1 Dec 1978	72	9.8	9.4	9.2
northern winter	19 Jan 1979	96	10.1	9.8	9.6

Table 3. *Root mean square vector wind errors (summer)*

Region	Domain/period	Forecast hour	Barotropic model	One-level PE model	Persistence
III	120°W–75°W	24	3.16	3.01	3.07
Central America	20.625°S–29.375°N	48	4.82	4.12	4.08
	15 June–15 Sept 1979	72	5.24	4.57	4.41
		96	5.38	4.80	4.43
IV	120°W–75°W	24	3.78	3.31	3.48
Western Atlantic	20.265°S–39.375°N	48	5.20	4.29	4.64
South America	15 June–15 Sept 1979	72	5.48	4.67	4.92
		96	5.53	4.74	4.82
V	100°W–38°E	24	4.82	4.97	5.47
West African	25°S–45°N	48	6.15	6.02	6.50
monsoon	16 June–15 Sept 1979	72	6.87	6.31	6.49
		96	7.09	6.44	6.66
VI	30°E–90°E	24	5.13	4.84	4.09
Indian summer	30°S–39.375°N	48	7.15	6.10	5.43
monsoon	1 June–31 July 1979	72	8.64	6.97	6.05
		96	9.30	7.79	6.34
VII	90°E–150°E	24	4.51	4.53	4.25
summer monsoon	30°S–39.375°N	48	6.61	5.97	5.76
over South-east	1 June–31 July 1979	72	7.30	6.86	6.48
asia		96	7.52	7.35	6.72

from the local zonal flows as they propagate westward (Tripoli and Krishnamurti, 1975). Beyond 48 h, the deterioration of the barotropic forecast over this region is attributed to a collapse of the basic zonal easterlies and the West African monsoon. Adiabatic models cannot sustain a source of energy for the African monsoons on a time frame beyond 2 days (Krishnamurti et al., 1979).

The failure of the simple barotropic model over most regions appears to be due to the crucial role of convection and associated divergent motions. The lowest skill of the model was noted over the winter monsoon regions where the diabatic processes and divergent circulations are dominant.

The single level primitive equation model performs better than the simple vorticity conserving model in all regions. However, useful skill is exhibited only over the following regions:

Region II	Central Pacific Ocean during northern winter to 1 day.
Region III	Central American during northern winter to 1 day.
Region IV	Western Atlantic and South America during northern summer to 4 days.
Region V	West African monsoon and Eastern Atlantic during northern summer to 4 days.

The performance over the Asian monsoon regions is generally quite poor, where the role of diabatic heating and divergent motions are dominant. The results over the Atlantic Ocean, South America and West Africa do seem to suggest the practical utility of the single level primitive equation model. Fig. 2 (a, b, c) shows an illustration of a 96-h wind forecast over the African Atlantic region during northern summer. The top panel illustrates the observed while the bottom panel shows the predicted motion field at 700 mb for hour 96. The trough lines of the African and Atlantic waves are shown by heavy lines.

4. Towards optimization of the single-level primitive equation model

An experimental domain extending from 30°E to 150°E and 11.25°N to 71.25°N was used for the optimization of the single level primitive equation model. At first we carried out prediction experiments at the 700 mb surface utilizing once daily observations starting at 0000 GMT. Initialization, as before, was carried out solving the reverse balance equation followed by a dynamic initialization. In a first series of experiments (for May 1979) the mean free surface height, $\overline{H}$, was limited to 2 km while the maximum height, h_{max}, of the orography was limited to 1 km. Results of evaluation of 96-h forecast showed that the rms vector wind error over China at 24 h was comparable to the persistance error. Thus almost no useful skill was evident over a domain enclosed within 20°N to 60°N, 70°E to 140°E.

A further series of experiments were next carried out varying the parameters $\overline{H}$ and h_{max}. In this parameter space, 700 mb forecasts do show skill, even at 96 h. The results, of skill, based on a very large number of experiments are summarized in Table 4. This shows that during the month of May 1979 an optimal choice of parameters $\overline{H}$ and h_{max} does lead to a major improvement of the overall wind forecast skill at 700 mb. However when we examined the prediction experiments individually for the optimal values of $\overline{H}$ and h_{max} we noted that the skill varies during this month. Higher skill was noted for experiments whose initial states were selected during the middle period May 11 through 25, 1979. On the other hand the prediction skill was much lower, for experiments that began during May 1 through 7, 1979 and May 26 through 29, 1979. Fig. 3 illustrates the mean 700 mb flows for the aforementioned three periods. It is interesting to note here that the flows are less zonal with strong motions normal the boundaries for the periods May 1 to May 7 and May 26 to May 29, 1979. On the other hand the flows are more nearly zonal during the period of improved skill, i.e., May 11 to May 25, 1979. Fig. 4 (a, b, c) respectively illustrates the initial state, a 96-h wind forecast and the verification (observed) winds at hour 96 during the period. These forecasts were made at 700 mb. It illustrates a rather substantial change in the 700 mb flows during the four days over China and its reasonable prediction. The optimal parameters for this forecast were $\overline{H} = 10$ km and $h_{max} = 3$ km. The root mean square vector wind error on day 4 was 11.1 m/s while the persistance error was 11.9 m/s.

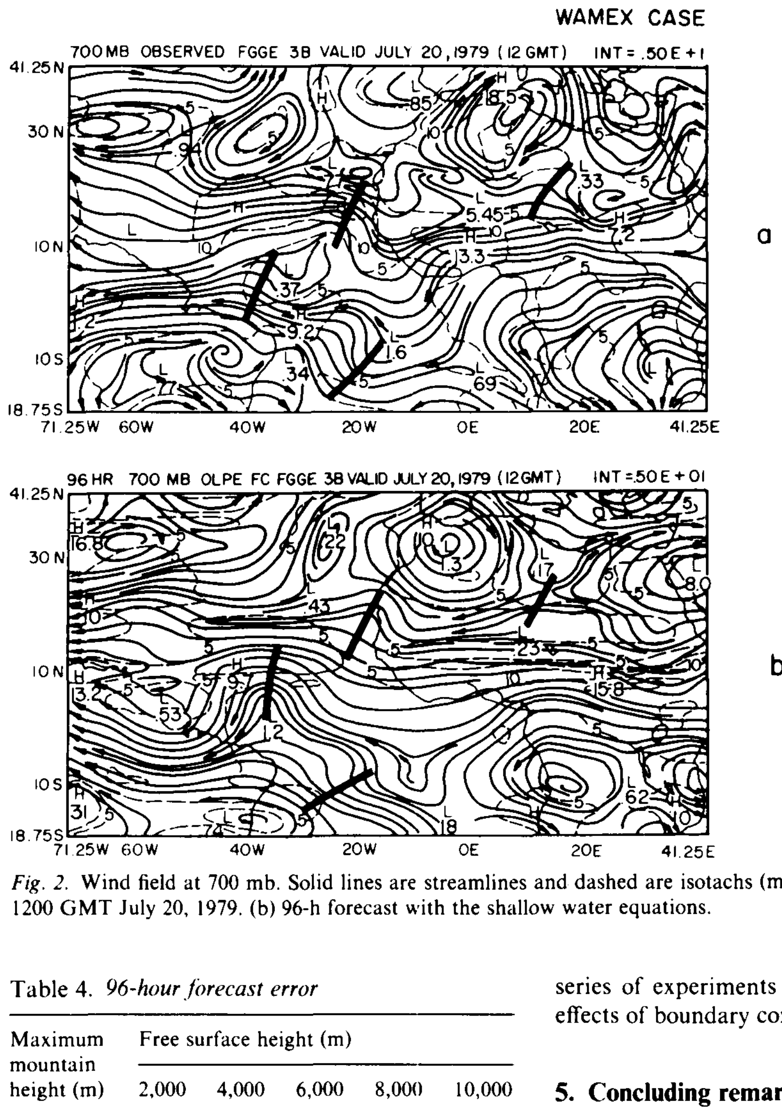

Fig. 2. Wind field at 700 mb. Solid lines are streamlines and dashed are isotachs (m s^{-1}). (a) Observed wind field 1200 GMT July 20, 1979. (b) 96-h forecast with the shallow water equations.

Table 4. *96-hour forecast error*

Maximum mountain height (m)	Free surface height (m)				
	2,000	4,000	6,000	8,000	10,000
500	11.6	11.0	11.0	10.9	10.8
1,000	11.9	11.2	11.1	11.1	11.0
2,000		11.6	11.3	11.1	11.0
3,000		11.9	11.5	11.2	11.1
4,000			11.5	11.3	11.1
5,000			11.7	11.3	11.1

Persistence error. 11.9.

The initial state, over the limited domain, appears to be another factor that seems to limit the quality of prediction especially for the choice of boundary conditions adopted here. Further series of experiments are needed to explore the effects of boundary conditions and initial states.

5. Concluding remarks

An optimization of the single level primitive equation appears to be possible from a careful choice of two parameters, i.e., the mean height of the free surface and the maximum height of the bottom topography. That avenue of investigation produced improved results over a domain enclosing China. The improvement was quite marked during a 15-day period in May 1979. Further experimentation over different domain and different initial states remains to be carried out.

At first we carried out well over 500 experiments over different tropical domains to assess

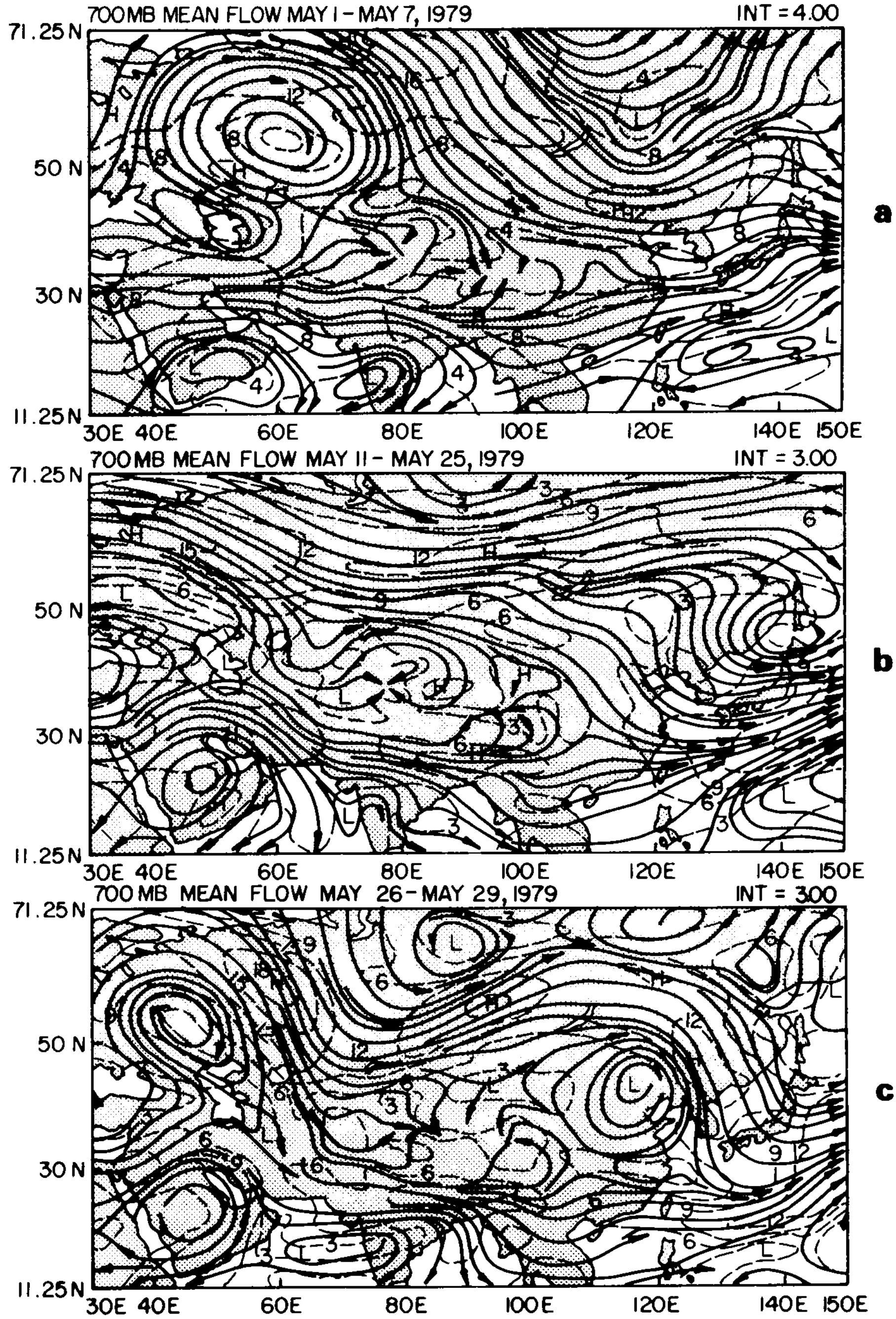

Fig. 3. Average flow field at 700 mb. Solid lines are streamlines and dashed are isotachs (m s^{-1}). Top panel: the period May 1 through May 7, 1979. Middle panel: the period May 11 to May 25, 1979. Bottom panel: the period May 26 to May 29, 1979.

the skill for a fixed choice of these parameters, i.e., free surface height of 2 km and the maximum orographic height of 1 km. That choice produced the best results over West Africa

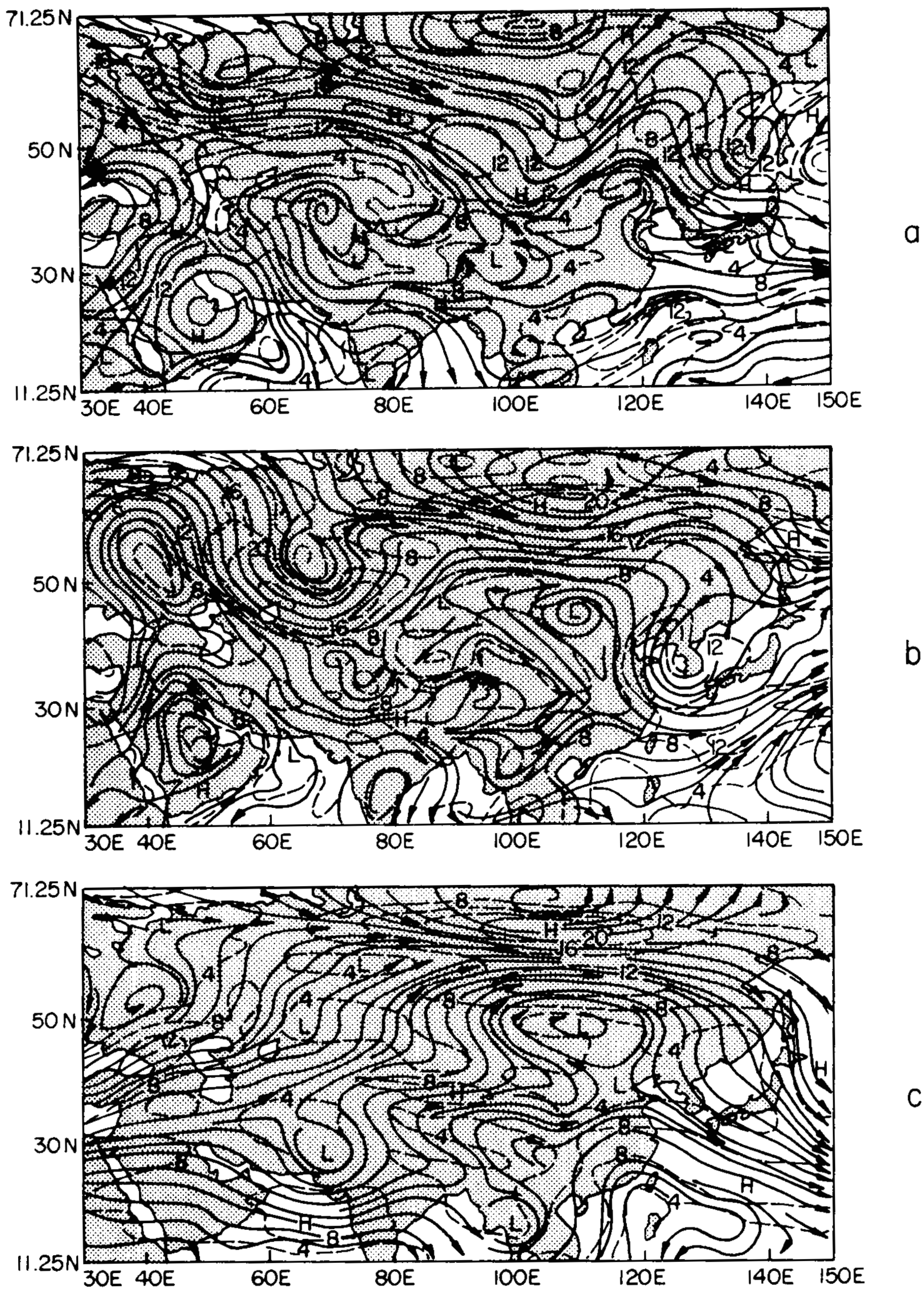

Fig. 4. Flow field at 700 mb. Solid lines are streamlines and dashed are isotachs (m s^{-1}). (a) Observed flow field 0000 GMT Dec 21, 1979. (b) Observed flow field 0000 GMT Dec 25, 1979. (c) 96-h prediced flow field valid at 0000 GMT Dec. 25, 1979.

and the Eastern Atlantic Ocean. Over these regions the root mean square vector wind error was slightly smaller than the persistance error in the time frame of 3 to 4 days. That, we believe, may be related to the barotropic energy source for the African waves in the low-level easterly jet.

6. Acknowledgements

The research reported here was supported by KRIS ATM-8304809-02, the National Science Foundation and NOAA NA82AA-D-00004, the National Oceanic and Atmospheric Administration. The computations were performed on the Harris 100 computer of the Department of Meteorology at Florida State University, Tallahassee, Florida. The assistance from our colleagues Yap, Atma, Tint, Joseph Adejokun and Chris Zelzer is gratefully acknowledged.

REFERENCES

Adejokun, J. A. and Krishnamurti, T. N. 1983. Further numerical experiments on tropical waves. *Tellus 35A*, 398–416.

Arakawa, A. 1966. Computational design for longterm numerical integration of the equations of atmospheric motions. *J. Comp. Phys. I*, 119–143.

Krishnamurti, T. N. 1962. Numerical integration of primitive equations by a quasi-Lagrangian advective scheme. *J. Appl. Meteorol. 1*, 500–521.

Krishnamurti, T. N. and Pearce, R. P. 1977. The fundamentals of numerical weather prediction and the filtered barotropic model. Proceedings of WMO Seminar, DAKAR, November 1976, WMO, Report No. 492. Geneva, Switzerland.

Krishnamurti, T. N., Pan, H. L., Chang, C. B., Ploshay, J., Walker, D. and Oodally, A. W. 1979. Numerical weather predictions for GATE. *Q. J. R. Meteorol. Soc. 105*, 979–1010.

Krishnamurti, T. N., Pasch, R. J. and Ardanuy, P. 1980. Prediction of African waves and specification of squall lines. *Tellus 32*, 215–231.

Mathur, M. B. 1970. A note on an improved quasi-Lagrangian advective scheme for primitive equations. *Mon. Wea. Rev. 98*, 214–219.

Matsuno, T. 1966. Numerical integration of primitive equations by a simulated backward difference method. *J. Meteorol. Soc. Japan 44*, 76–84.

Pedlosky, J. 1979. *Geophysical Fluid Dynamics*. Springer-Verlag, New York.

Ploshay, J. J. 1977. Results of single level numerical prediction experiments during GATE. Masters Thesis, Florida State University, Tallahassee, Florida. 32306, USA.

Rennick, M. A. 1976. The generation of African waves. *J. Atmos. Sci. 33*, 1955–1969.

Tripoli, G. and Krishnamurti, T. N. 1975. Low level flows over GATE area during summer 1972. *Mon. Wea. Rev. 103*, 197–216.

Williamson, D. L. 1976. Normal mode initialization procedure applied to forecasts with global shallow water equations. *Mon. Wea. Rev. 104*, 195–206.